Kahramanmaras Sutcu Imam University
Journal of Engineering Sciences

HARRAN EVİ GEOMETRİSİNİN BİNA ISIL PERFORMANSI ÜZERİNDEKİ ETKİSİNİN DENEYSEL OLARAK İNCELENMESİ

EXPERIMENTAL INVESTIGATION OF THE EFFECT OF HARRAN HOUSE GEOMETRY ON BUILDING THERMAL PERFORMANCE

Erdal YILDIRIM (ORCID: 0000-0002-9309-2420)

Harran Üniversitesi Organize Sanayi Bölgesi Meslek Yüksekokulu 63200, Şanlıurfa

*Sorumlu Yazar / Corresponding Author: Erdal YILDIRIM, erdaly@harran.edu.tr

ÖZET

Bu çalışmanın amacı yaz aylarında iç ortam havasını daha serin tutan Harran konik çatılı evlerini enerji verimliliği açısından, bina çatı geometrisinin iç ortam havasına etkisini araştırmaktır. Bu amaçla Harran konik çatılı evler aynı taban alanı, hacim ve termofiziksel özelliklere sahip düz çatılı bir bina ile karşılaştırılmıştır. Farklı geometrilerdeki çatılardan gerçekleşen ısı transferiyle bütün binanın ısıl performansını değerlendirmek amacıyla deneysel bir çalışma gerçekleştirilmiştir. Bu çalışmanın amacı, hangi çatı geometrisinin yaz mevsiminde daha enerji verimli olduğunu belirlemektir. Bu sebeple düz çatılı bina referans alınarak farklı geometrideki çatılarla karşılaştırılmıştır. Adyabatik hazne tekniği kullanılarak çatı tiplerinin doğal ısı transfer katsayıları ve toplam ısı transfer katsayıları deneysel olarak incelenmiştir. Sonuç olarak konik çatılı modelin dış yüzey doğal taşınım ısı transfer katsayısının ve toplam ısı transfer katsayısının düz çatıya göre sırasıyla 1,5 ve 2,5 kat daha fazla olduğu bulunmuştur. Bulunan sonuçlar, yaz aylarında Harran evlerinde iç hava sıcaklığının daha düşük olmasını doğrular niteliktedir.

Anahtar Kelimeler: Doğal taşınım, çatı geometrisi, toplam ısı transfer katsayısı

ABSTRACT

The aim of this study is to investigate the effect of building roof geometry on indoor air in terms of energy efficiency in Harran conical roof houses, which keep indoor air cooler in summer. For this purpose, Harran conical roof houses were compared with a flat roofed building with the same floor area, volume and thermophysical properties. An experimental study was carried out to evaluate the thermal performance of the whole building with heat transfer from roofs of different geometries. The aim of this study is to determine which roof geometry is more energy efficient in summer. For this reason, the flat roofed building was compared with roofs of different geometry. The natural heat transfer coefficients and total heat transfer coefficients of the roof types were investigated experimentally by using the adiabatic chamber technique. As a result, the outer surface natural convection heat transfer coefficient and the total heat transfer coefficient of the conical roof model were found to be 1.5 and 2.5 times higher, respectively, than the flat roof. The results found confirm that the indoor air temperature is lower in Harran houses during the summer months.

Keywords: Natural convection, roof geometry, total heat transfer coefficient

| KSÜ Mühendislik Bilimleri Dergisi, 25(2), 2022 | 96 | KSU J Eng Sci, 25(2), 2022 |
| Araştırma Makalesi | | Research Article |

E. Yıldırım

GİRİŞ

It is known that conical domed Harran houses keep the indoor air cooler in summer than modern flat-roofed buildings (Basaran, 2011; Yildirim et al., 2014). Experimentally examining the effect of domed roof geometries on the indoor environment and reflecting their advantageous effects on new building designs is important in terms of energy savings. There are many studies in the literature on the investigation of natural convection in closed spaces, which are associated with many other engineering and industrial applications such as electronics, room heating, solar collectors (Sarris et al., 2004; Dalal & Das, 2006; Dogan et al., 2012; Saleh & Hashim, 2014).

Computational fluid dynamics (CFD) simulations are frequently used in analyzes where the effect of building geometry on the convection heat transfer coefficient (CHTC) is investigated. Hu et al., (2018) investigated the convective heat transfer coefficient on different building surfaces and ground for a building cluster with high Reynolds number. Forced, natural and mixed convection heat transfer states are simulated. Surface-averaged Nusselt numbers for forced convection were found to be proportional to $Re^{0.79}$. The Nusselt numbers are the windward, upper, side, leeward surface and ground numbers, respectively, from largest to smallest. For natural convection, surface-averaged average Nusselt numbers were found to be proportional to $Gr^{1/3}$. Nusselt numbers were found as wall, surface and floor numbers, from largest to smallest, respectively. Montazeri & Blocken, (2018) investigated the combined effects of wind speed, building height and width, and wind direction on the surface-averaged $CHTC_{avg}$ for windward facades of buildings. High resolution CFD simulations of wind flow and forced convection heat transfer were performed and validated by wind tunnel measurements. The results show that $CHTC_{avg}$ for a given wind direction increases as the building height increases. However, increasing the building width has the opposite effect on $CHTC_{avg}$. Montazeri & Blocken, (2017) derived new generalized expressions from CFD simulations for surface-averaged forced convection on building facades and roofs, taking into account the reference wind speed, the width and height of the building facade against the wind as parameters. The results show that for a given building geometry, the relationship between surface-averaged convection heat transfer coefficient and wind speed is an exponential power law dependent on the surface type (upwind, lee, side, face, roof). In another study (Montazeri et al., 2015) in which the effect of building size and geometry on the heat transfer coefficient was examined, CFD simulations of forced convection heat transfer was carried out on the windward facade of 22 buildings with different geometries. The effect of the building geometry on the convective heat transfer coefficient distribution was investigated at different reference wind speeds: for buildings with H≥W, for buildings with H≤W and for buildings with H=W. The results show that $CHTC/U_{10}^{0.84}$ is relatively insensitive to the reference wind speed. For W=10 m and increasing H from 10 m to 80 m, the surface-averaged $CHTC/U_{10}^{0.84}$ on the wind direction front increases by about 20%. However, for H=10 m, increasing the building width from 10 to 80 m has the opposite effect on the surface-averaged $CHTC/U_{10}^{0.84}$. Jiang et al., (2020) used CFD simulations to analyze the forced convection heat transfer in the louvered wind front, which was confirmed by wind tunnel experiments. In most cases, the surface average convection heat loss of sun-side louvers is much higher than that of the shaded side. The maximum difference was found more than twice.

In the literature, there are studies in which alternative and new approaches are tried in studies examining the relationship between building geometry and heat transfer coefficient. François et al., (2020) presented an alternative approach to estimate the value of the whole building by determining the heat flux at a particular location on the wall surface. As a result of the method used, h coefficient values close to and similar to the standard value in ISO 14683 standards were found. Yang et al., (2017) determined the radiative heat flux, convective heat flux, and total received heat flux on the outer surface of an exterior wall in different seasons with an experimental approach. The results show that radiation heat accounts for a large portion of the total heat throughout the year. In the study (Evangelisti et al., 2017), in which heat transfer processes between building walls and the environment were examined using on-site measurements, existing correlations based on wind speed, Standard recommendations and an empirical methodology, there was a percentage difference of 26.5% with the Standard and 13.4% with the ASHRAE correlation. found.

There are also studies in which building geometry and energy consumption, heat transfer coefficients are carried out with theoretical analyzes and different simulation software. The total and radiative heat transfer coefficients of an enclosure with different room sizes, heated from a single wall, were investigated by theoretical calculations and the Engineering Equation Solver (EES) program. A correlation was found that includes the effect of aspect ratio (H/L). The results showed that the average radiation coefficient is in the range of 5.4-5.5 W/m^2 K and it changes little according to the room dimensions (Acikgoz, 2015). This study presented an approach for calculating heat

KSÜ Mühendislik Bilimleri Dergisi, 25(2), 2022	97	KSU J Eng Sci, 25(2), 2022
Araştırma Makalesi		Research Article

E. Yıldırım

emissions from buildings to ambient air and applied the approach in EnergyPlus. A simplified spreadsheet calculation has been made to validate the method implemented in EnergyPlus. Hong et al., (2020) conducted simulations covering 16 commercial building types, four climates and two energy efficiency levels to understand and evaluate building heat emissions. The simulation results showed that the annual site energy use of a building is different from the annual heat emissions. In 70% of the simulations, heat emissions were higher than on-site energy use. For most building typologies, it is concluded that climate has a strong influence on heat emissions. Iousef et al., (2019) investigated the effect of external CHTC models on the predicted energy performance of buildings with a wide variety of geometries. EnergyPlus six commonly used CHTC models are applied and compared. While there is a deviation of -14.5% for the annual heating demand, a maximum deviation of +42.0% is obtained for the annual cooling demand compared to the generalized CHTC model. Premrov et al., (2017) focused on the impact of building shape on annual energy needs in six different macro-climate regions in Europe. As a result, it was found that two-storey houses outperform single-storey houses in cold climate conditions. The increased aspect ratio has a positive effect on reducing the energy requirement. In the case of hot climatic conditions, the findings were almost the opposite of those obtained for cold climes.
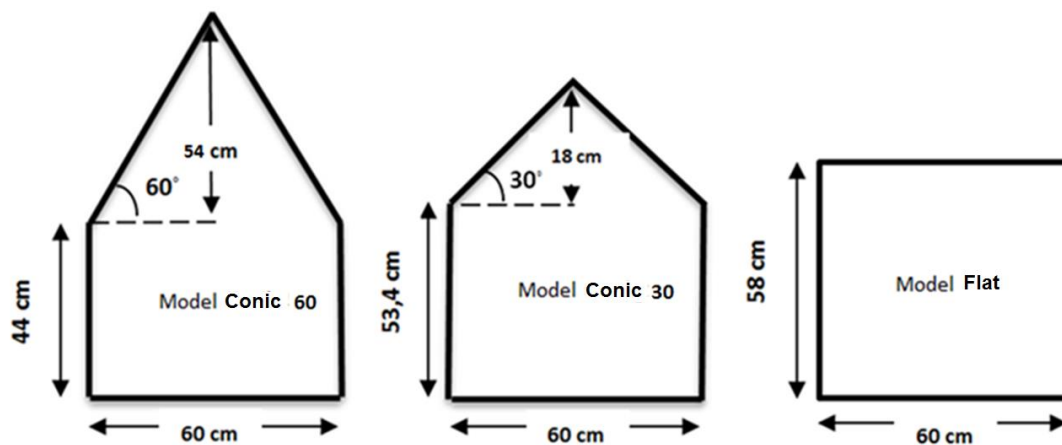
Before the experimental work presented in this study, CFD simulations were performed for the same scenario. Harran's conical roofed building has for this purpose been compared with flat roofed building of equivalent thermo-physical properties, base area and volume (Yildirim et al., 2017). Three dimensional CFD simulations using the low-Reynolds number modeling (LRNM) and standard turbulence models are performed. The effect of roof geometry on natural ventilation is investigated. The conical roof house has higher convective heat transfer coefficient on windward side but a lower value on the roof. In the case of wind incidence angle of 90 and cross ventilation, the Harran house has better (8%) performance than flat roofed building.

The literature review clearly shows that the effects of building geometry on thermal performance have been the subject of many studies, but the relationship between natural convection and roof geometry has not been closely examined. In this study, the U-value approach, which covers all the effects of heat transfer from the roof, including convection, conduction, and radiation, was used. In order to determine which of the roof geometries is more resistant to heat loss, it was investigated experimentally using the adiabatic box technique (Yesilata & Turgut, 2007; Turgut & Yesilata, 2009). The thermal performances of different roof geometries have been determined by assuming the same volume and floor area. The walls and floors of the models are insulated, only the roof is made of metal, and the direct effect of the roof geometry on the indoor air and the natural convection from the roof are examined. The values obtained by the method used were validated with the literature values.

METHOD

Preparation of Building Models

The Conic 60 building model is a 1/5 reduced dimensions of an actual Harran house room. Model Conic 30 and Flat have same volume and base area with Model Conic 60 (Figure 1).

Figure 1 The Building Models and The Roof Angles Used in Experiment

| KSÜ Mühendislik Bilimleri Dergisi, 25(2), 2022 | 98 | KSU J Eng Sci, 25(2), 2022 |
| Araştırma Makalesi | | Research Article |

E. Yıldırım

As can be seen from Figure the roof slope of Model Conic 30 and 60 are respectively 30° and 60°. Walls and floors of the models are constructed from 15 cm expanded polystyrene has a thermal conductivity of ~0.040 W/m K. 1.5 cm galvanized iron sheet used for roofs and has thermal conductivity of 15.6 W/m K (Figure 2).
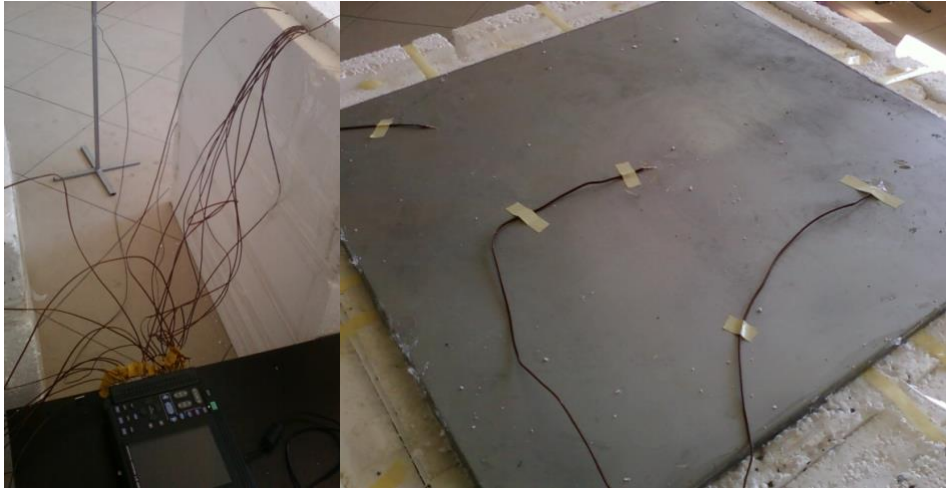

Figure 2 Model Conic 30, Flat and Conic 60

Figure 3 Water Reservoir with Resistance Heater and Placing on The Floor Closed with Aluminum Foil

30 lt of water put into reservoir made of sheet metal and closed with aluminum foil (Figure 3) Once the roof placed on the walls, the junctions were sealed with silicone adhesive to prevent indoor air leakage.

Measuring Instruments

Temperature measurement is made by using T-type thermocouple in experiments. Read error is about ±0.25°C with the thermocouple. The temperature measurement points are shown in Figure 5. Also, the ambient and the wall surface temperatures of the room are measured. Temperature measurements were made at intervals of 10 minutes and saved with 32 Channels Hioki 8422-51 Memory Hilogger (Figure 4).

| KSÜ Mühendislik Bilimleri Dergisi, 25(2), 2022 | 99 | KSU J Eng Sci, 25(2), 2022 |
| Araştırma Makalesi | | Research Article |

E. Yıldırım

Figure 4 The Data Logger Used in Experiments and the Placement of the Thermocouples on the Outer Surface of Model Roofs

Measurements and Assumptions

Water in the reservoir is heated to a certain temperature and the electrical connection is cut off then the water is allowed to cool. Experiments were made in a closed space. During experiments average of the difference between the wall outside surface temperatures of the models and the ambient temperature are observed about 0.5°C. The temperature gradient is assumed to be along the y axis and in the horizontal (x axis) it is negligible (Figure 5). For the surface temperatures, measurements were made at many points. And then the average of the measured values used in calculations as an isothermal surface. The indoor air temperatures of the models are the average of measurements at six different points as shown in Figure 5.
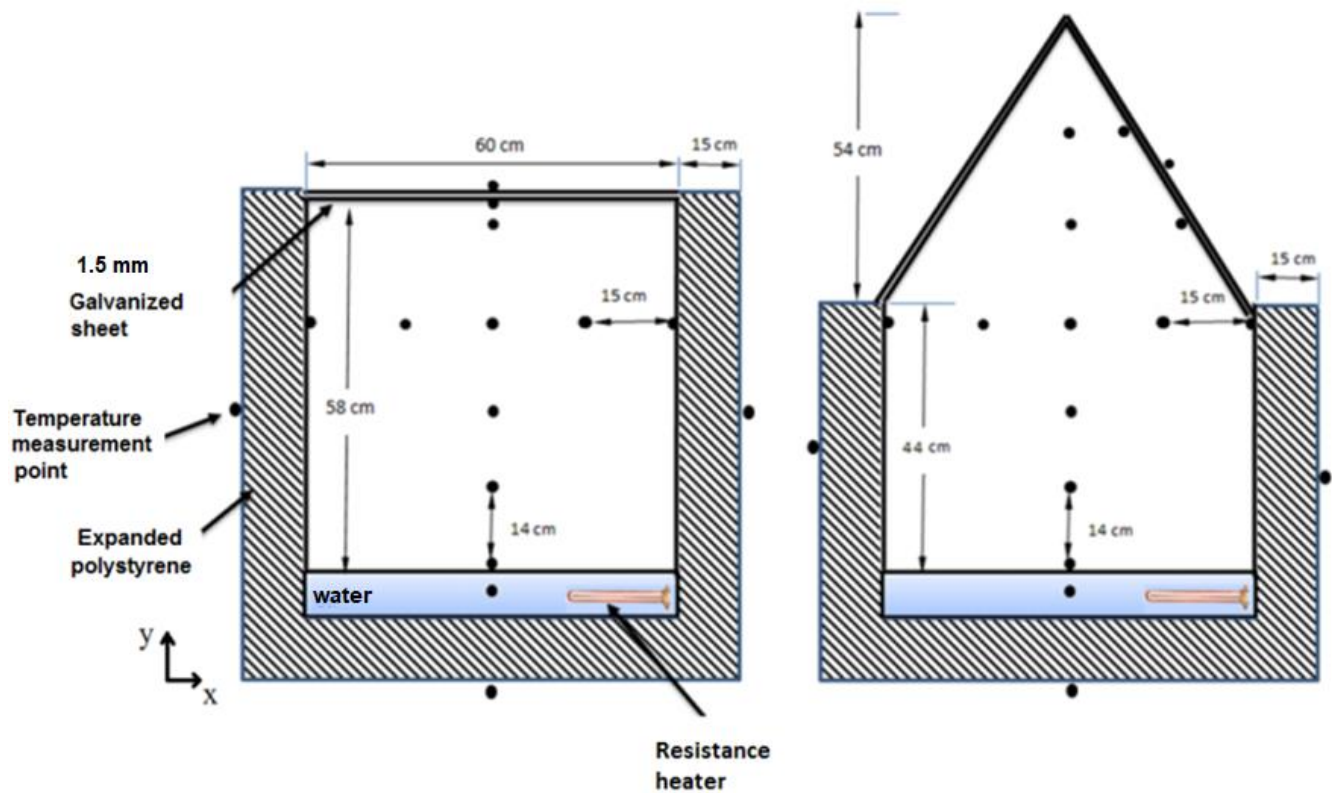
Figure 5 The Experimental Setup Belonging to Model Flat, Conic 60 and Temperature Measuring Points

Two methods are used to examine the data obtained from the measurements. These are dimensionless temperature and energy balance method

## Dimensionless Temperature Method

Testing of the building models are not carried out at same time so the outdoor temperatures of models may be different. Similarly, the water temperature in the reservoir in the beginning of the test may vary slightly according to the model. To eliminate these differences between the models and to make an objective approach the dimensionless temperature method is used. The equilibrium temperature could not be obtained although experiments last more than 24 hours. This definition is useful even for building models tested at different indoor and outdoor temperatures while maintaining the same heat transfer mechanism. Since the rate of reduction of the curves at the end of the experiments is almost constant, the experimental period can be considered long enough to make a fair comparison. (Turgut & Yesilata, 2009). The dimensionless temperature is defined as below,

$$\theta^* = \frac{T(t)-T_0}{T(t=0)-T_0}$$
(1)

where, $T(t = 0) = T_i$ is initial temperature of water and $T(t)$, is temperature of reservoir at any time 't' and T_0 is the ambient temperature. Thus, it will be possible to compare insulating properties of different roof geometries by these dimensionless temperature parameters.

Energy Balance Method

In the literature (Globe & Dropkin, 1954) there are relations for horizontal rectangular closed spaces with surfaces at constant temperature. When the hot plate is at the bottom, significant convection currents start for $Ra_L > 1708$ and the heat transfer rate increases (Figure 6). Main objective is to determine the effects of heat transfer in the cavity (Nogueira et al., 2011). By this method, the total heat transfer coefficient and the convection heat transfer coefficients of each model's inner volume and external roof surface can be calculated. The calculation procedure is based on the energy balance applied to the roof of each model. The total heat transfer (Eq.2) taking place to the ambient air from the roof surface consists of convection (Eq.3) and radiation (Eq.4) (Figure 6)
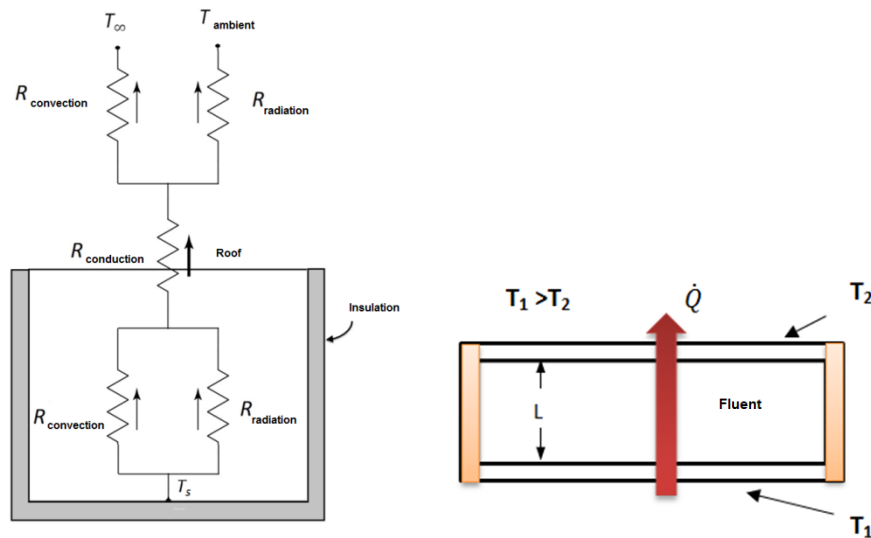
Figure 6 The Schematic Representation of The Convection and Radiation Resistances of Flat Roofed Model and a Rectangular Shaped Closed Environment Heated from Bottom Surface

$$q_{total} = q_{r,c} + q_{r,ra}$$
(2)

$$q_{r,c} = h_r\,(T_{o,s} - T_{ambient})$$
(3)

$$q_{r,ra} = \varepsilon\sigma(T_{o,s}{}^4 - T_\infty^4)$$
(4)

KSÜ Mühendislik Bilimleri Dergisi, 25(2), 2022
Araştırma Makalesi

101

KSU J Eng Sci, 25(2), 2022
Research Article

E. Yıldırım

where σ is Stefan-Boltzmann constant. Here the total heat transfer (q_{total}) is equal to heat transfer by conduction through the roof and therefore the natural convection heat transfer coefficient on the outer surface of the roof (h_r) can be calculated by the equation below,

$$h_r = \frac{k_r \frac{T_{i,s}-T_{o,s}}{L_{çr}} - \varepsilon\sigma(T_{o,s}{}^4 - T_\infty^4)}{(T_{o,s} - T_{ambient})}$$
(5)

where $T_{i,s}$ and $T_{o,s}$ are the temperature of inner and outer surface respectively. And the radiation heat transfer coefficient is calculated as,

$$h_{ra} = \varepsilon\sigma(T_{o,s}{}^2 + T_\infty^2)(T_{o,s} + T_\infty)$$
(6)

The temperature is Kelvin above equation, and it is observed that $T_{ambient} \approx T_\infty$ during experiments. The combined heat transfer coefficient is defined by

$$h_{combined} = h_r + h_{ra}$$
(7)

In literature there are many relations about natural convection heat transfer coefficients based on experimental studies (Cengel, 2011). Flat roof was evaluated as a cooling of horizontal hot upward plate. During the experiments Ra is observed in the range of $10^4 - 10^7$ and for this range, the relation (McAdams, 1954)

$$Nu = 0.54\, Ra_L^{1/4}$$
(8)

is used to calculate the average heat transfer coefficient on the external surface of the roof. Because of the heat transfer direction is vertical, the energy balance can be written between the ground and the roof. Total heat transfer taking place to roof consists of convection (Eq. 9), radiation (Eq. 10) and conduction (Eq. 11)

$$q_{c,in} = h_{in} * (T_s - T_{in,s})$$
(9)

where T_s and $T_{in,s}$ are the temperature of roof and inner surface respectively.

$$q_{ra,in} = \sigma * \frac{(T_s+273)^4 - (T_{in,s}+273)^4}{\left(\frac{1-\varepsilon_s}{\varepsilon_s}\right) + \left(\frac{1}{F_{12}}\right) + \left(\frac{1-\varepsilon_r}{\varepsilon_r}\right)}$$
(10)

where F_{12} is the view factor for parallel rectangles.

$$q_{con,in} = k_a * \frac{T_s - T_{in,s}}{L}$$
(11)

Therefore, the overall heat transfer from enclosure to roof is equal to the heat conduction through the roof and energy balance can be written as follows,

$$q_{c,in} + q_{rad,in} + q_{con,in} = k_r * \frac{T_{in,s} - T_{o,s}}{L_r}$$
(12)

The heat transfer coefficient for the enclosure can be obtained from the above equation and written as

$$h_{in} = \frac{k_r * \frac{T_{in,s}-T_{o,s}}{L_r} - \sigma * \frac{(T_s+273)^4 - (T_{in,s}+273)^4}{\left(\frac{1-\varepsilon_s}{\varepsilon_s}\right) + \left(\frac{1}{F_{12}}\right) + \left(\frac{1-\varepsilon_r}{\varepsilon_r}\right)} - k_a * \frac{T_s - T_{in,s}}{L}}{(T_z - T_{i,y})}$$
(13)

KSÜ Mühendislik Bilimleri Dergisi, 25(2), 2022	102	KSU J Eng Sci, 25(2), 2022
Araştırma Makalesi		Research Article

E. Yıldırım

In literature, there are also relations for the constant temperature rectangular enclosures (Cengel, 2011). As a result of flat roof model experiments, the range of Ra_L demonstrated compliance with the following equation (Globe & Dropkin, 1959) ($3x10^5 < Ra_L < 7x10^9$):

$$Nu = 0.069 \, Ra_L^{1/3} Pr^{0.074} \tag{14}$$

So, all the convection and radiation coefficients are known, the total thermal resistance from ground to roof of the models can be calculated as below,

$$R_{Total} = \frac{1}{h_{in}} + \frac{L}{k} + \frac{1}{h_o} \tag{15}$$

Uncertainty Analysis

Most widely used uncertainty analysis is the method of Kline and McClintock (1953). According to this method, R is the measured parameter and $x_1, x_2, x_3, \ldots \ldots, x_n$ are the independent variables. In this case, it can be written as below,

$$R = R(x_1, x_2, x_3, \ldots \ldots, x_n)$$
(16)

Each independent variable error rates are $w_1, w_2, w_3, \ldots \ldots, w_n$ and w_R is the error rate of R magnitude and is defined as,

$$w_R = \left[\left(\frac{\partial R}{\partial x_1} w_1 \right)^2 + \left(\frac{\partial R}{\partial x_2} w_2 \right)^2 + \cdots + \left(\frac{\partial R}{\partial x_n} w_n \right)^2 \right]$$
(17)

Errors in length measurement are neglected. Errors in temperature measurements depend on measurement instruments and as follows,

(k1) Uncertainty for thermocouple=±0.25°C
(k2) Uncertainty for data recorder=0.1°C
(k3) Uncertainty for the connections=0.1°C

Uncertainty in temperature measurement is calculated as follows,

$$w_T = [k_1^2 + k_2^2 + k_3^2]^{1/2} = \pm 0.28°C$$
(18)

Uncertainty in convection coefficients is calculated with the equation below,

$$\frac{w_h}{h} = \left[\left(\frac{w_Q}{Q} \right)^2 + \left(\frac{w_T}{\Delta T} \right)^2 + \left(\frac{w_{T\infty}}{\Delta T} \right)^2 \right]^{1/2}$$
(19)

where w_Q, is the uncertainty of conduction heat transfer and calculated as follows,

$$\frac{w_Q}{Q} = \left[\left(\frac{w_{T_{i,y}}}{\Delta T} \right)^2 + \left(\frac{w_{T_{d,y}}}{\Delta T} \right)^2 \right]^{1/2}$$
(20)

When the above equation solved for the conduction through the flat roof, $w_Q \cong \%8.1$ for $\Delta T = 5°C$. This high error rate is because of the small temperature difference. The temperature difference between the external surface of the roof and the ambient temperature is $\Delta T = 10°C$ and for this case $w_h \cong \% 9$. The uncertainty for Nusselt number can be calculated as below,

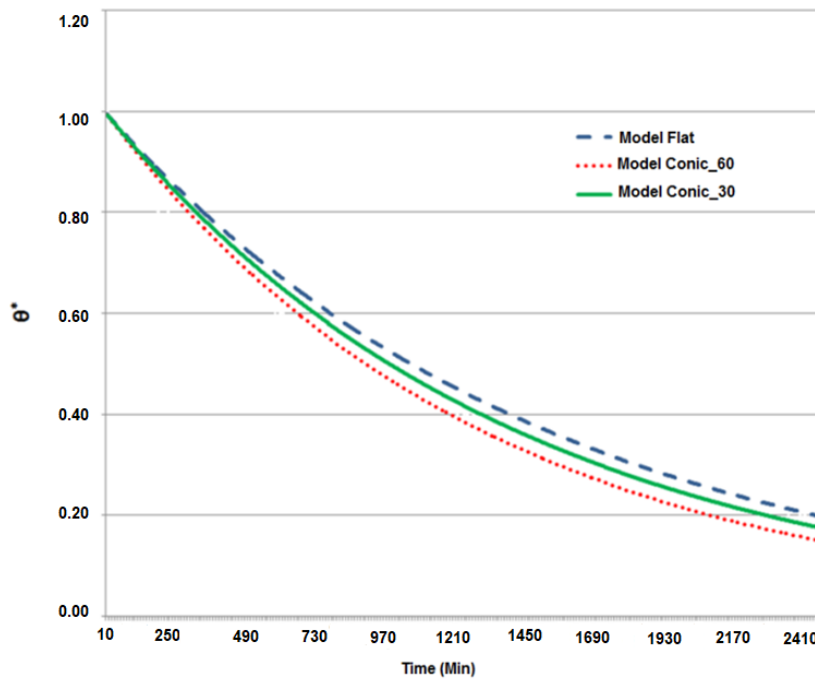$$w_{Nu} = \left[\left(\frac{L}{k} w_h\right)^2\right]^{1/2}$$
(21)

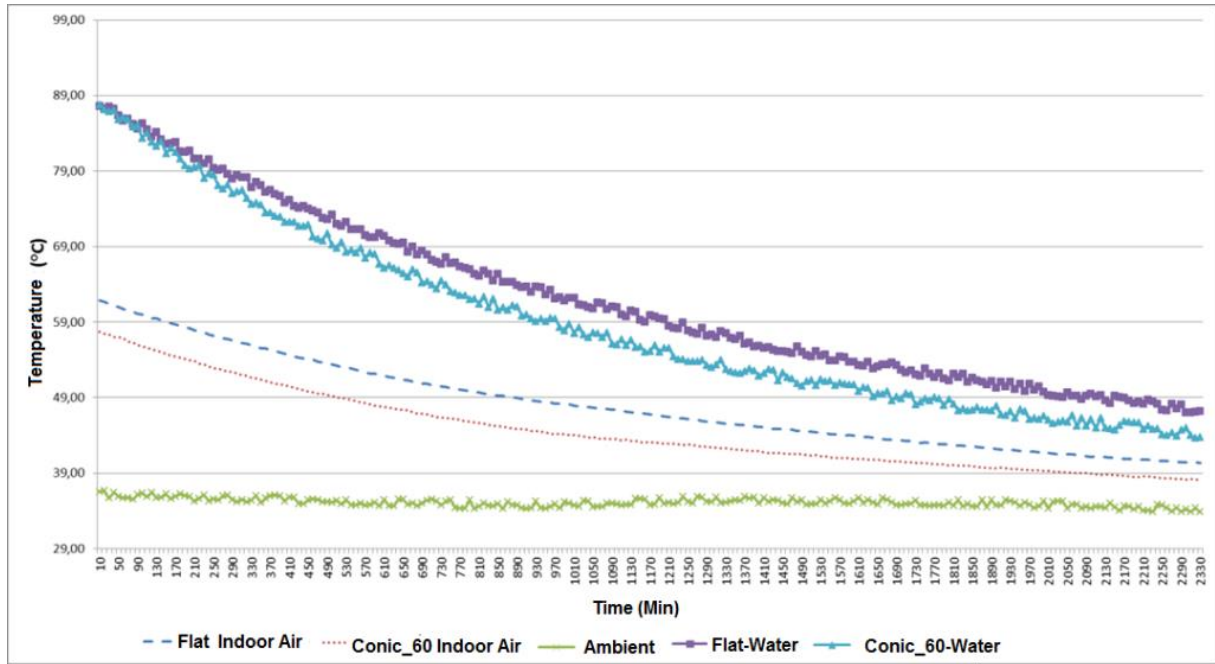The average convection coefficient of flat roof surface is $4.2\ W/m^2 K$, and the uncertainty for this value is about $w_{Nu} \cong \%2.1$

RESULTS AND DISCUSSION

As a result of experiments, the dimensionless temperature curves of the three roof models are drawn with using the obtained data. (Figure 7). As can be seen from the graph the flat roofed model is the most durable model in terms of losing indoor heat and the model Conic_60 tends to lose heat most quickly. Also Figure 8 is drawn for the comparison of the indoor air temperatures of the conical domed Harran house model (Conic_60) and the flat roofed model. At the same environment conditions, the water in the reservoirs of these two models is heated to same temperature (87.5 ℃) and allowed them to cool approximately 39 hours. As Figure 8 shows that Model Conic_60 indoor air temperature is 3.4℃ less than the flat roof model during the cooling period.

Figure 7 The Variation of Dimensionless Temperature Difference with Time

KSÜ Mühendislik Bilimleri Dergisi, 25(2), 2022   104   KSU J Eng Sci, 25(2), 2022
Araştırma Makalesi   Research Article
E. Yıldırım

Figure 8 The Change of Indoor Temperature of The Model Flat and Model Conic_60

To determine the effect of the roof geometry to indoor air, the total thermal resistances of the models are calculated (Table 1). The total heat transfer coefficient of the Model conic_60 is found the highest.

Table 1 Total Heat Transfer Coefficient of The Models

Model	U-value (W/m^2K)	R (K/W)
Flat	1.6	1.77
Conic_30	4.6	0.34
Conic_60	5.6	0.20
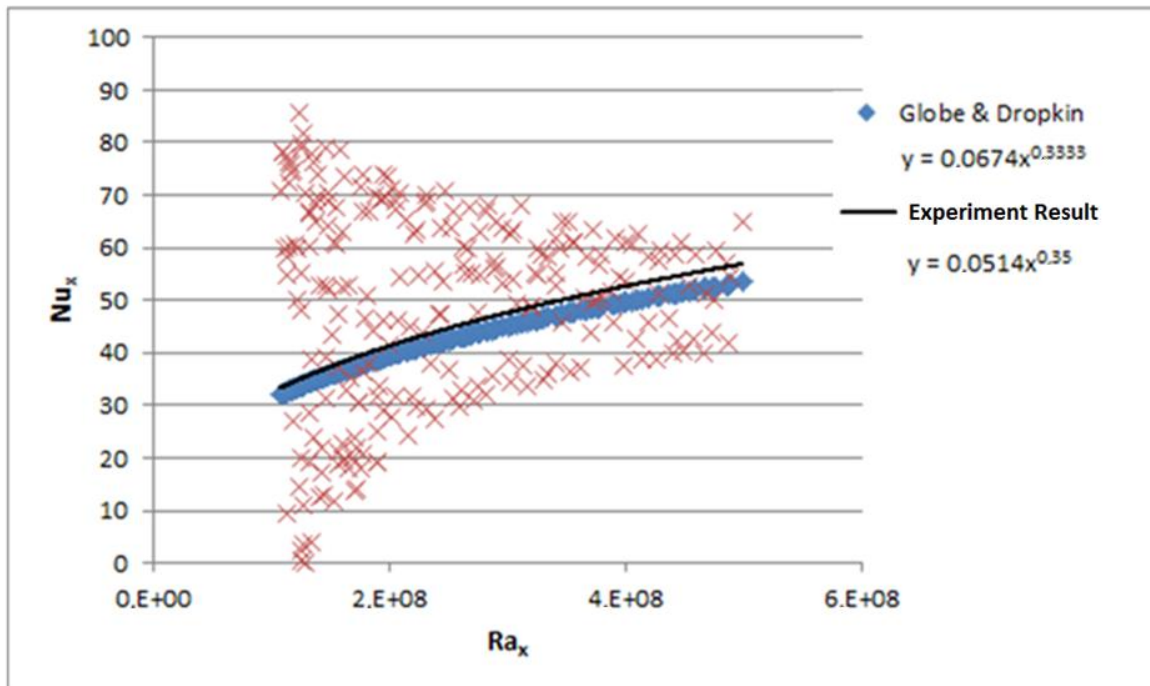
Figure 9 shows the comparison of the correlation given in literature for constant temperature horizontal enclosures and the flat roofed model experiment results. And Figure 10 shows the comparison of the correlation given in literature for cooling of constant temperature hot plate in a cold environment and the experimental results of the cooling of flat roof. As can be seen in Figure 9 and 10 the data obtained from the experiments fit to the slope of literature values. The average value of the natural convection heat transfer coefficient of the enclosure of the flat roof is found $1.9\ W/m^2K$ by using the literature correlation. As a result of experimental data, its average is found $1.8\ W/m^2K$.
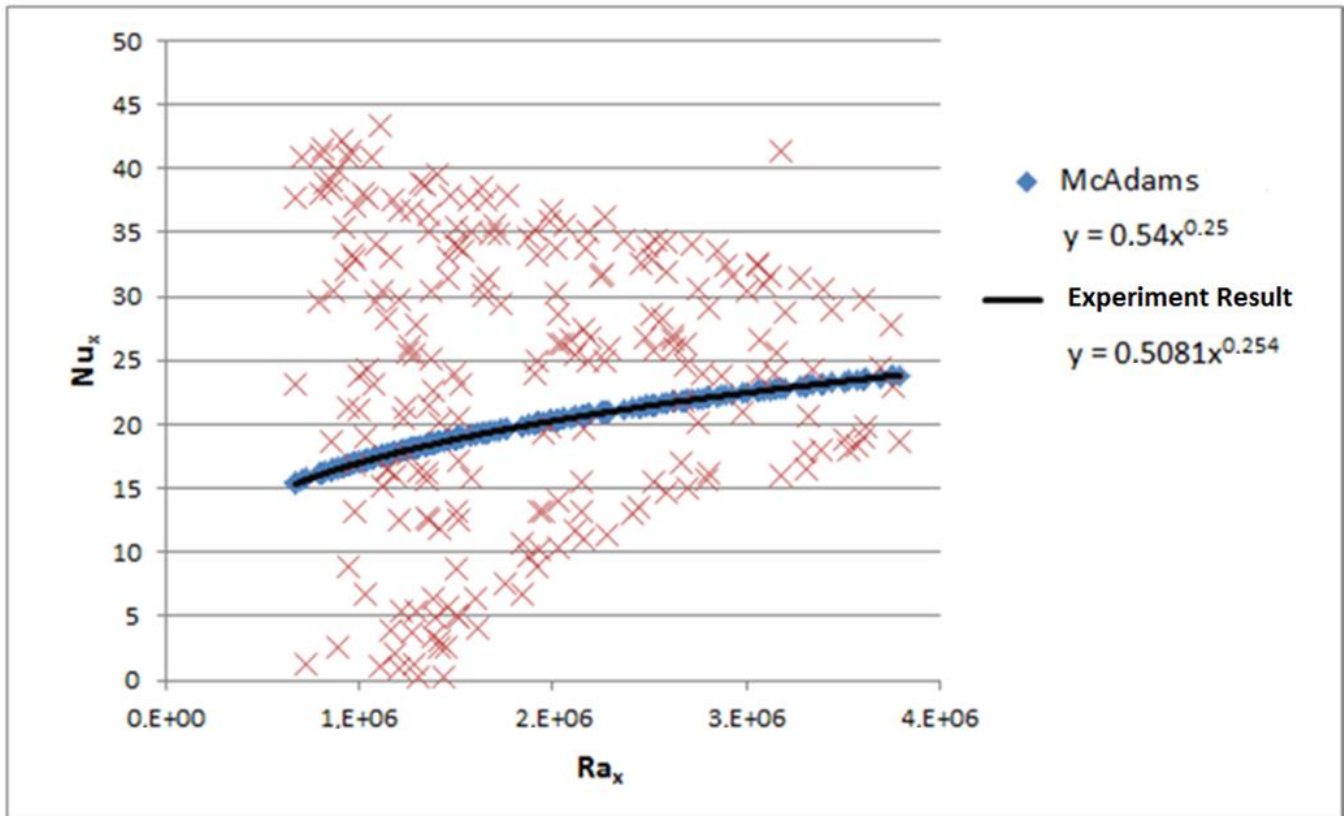

Figure 10 Comparison of Experimental Correlation with Correlation in Literature for The Average Nusselt Number of Natural Convection on a Horizontal Plate
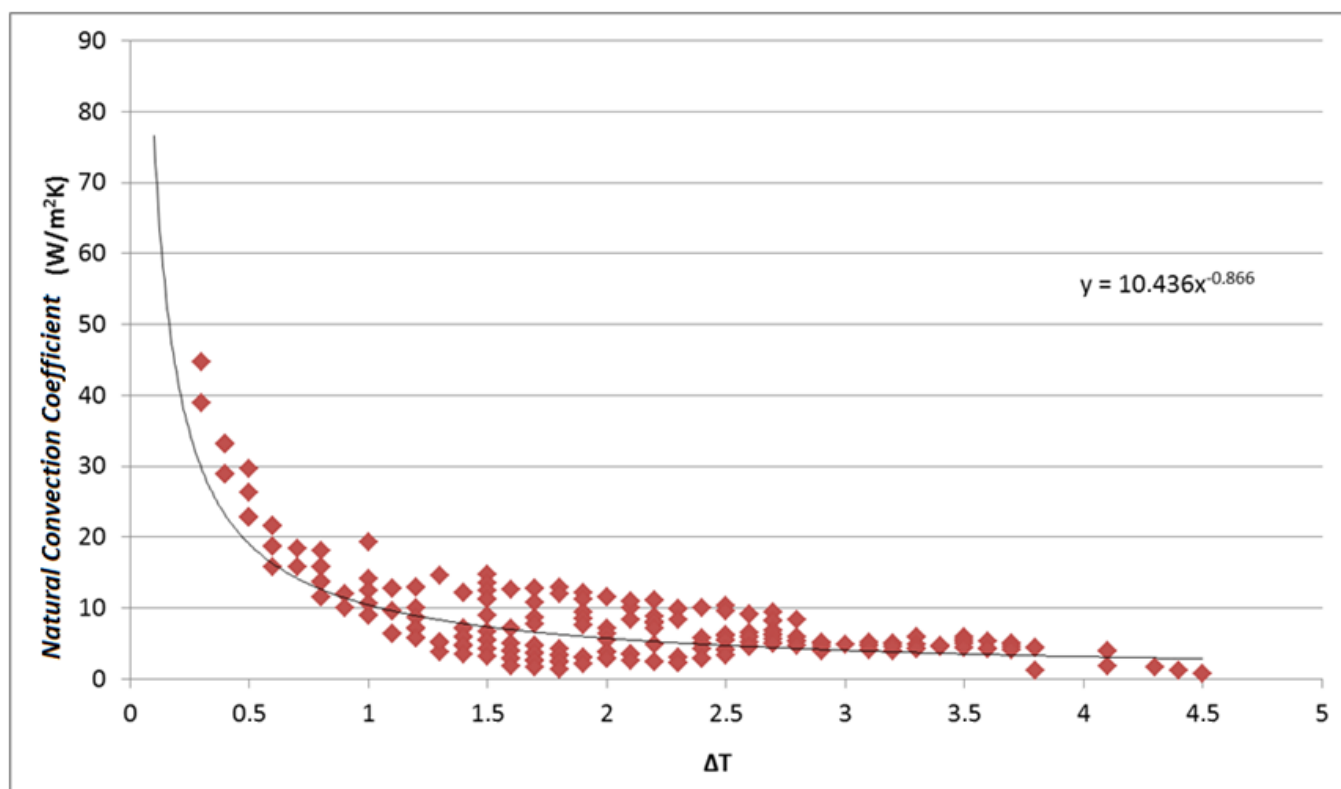
Figure 11, 12, 13 respectively show variation of the Conic_60, Flat, Conic_30 roof outer surface convection heat transfer coefficients as a function of the temperature difference between roof outer surface and the ambient temperature. The average natural convection coefficient of outer surface of Conic_60 roof is found $10.5\ W/m^2K$ and the value for indoor is $8.9\ W/m^2K$. The average of the flat roofed model roof outer surface convection coefficient is found $4.2\ W/m^2K$. The indoor average value of convection heat transfer coefficients of the flat roof is $1.8\ W/m^2K$ The average indoor and roof outer surface radiation heat transfer coefficients for flat roofed model is respectively $0.3\ W/m^2K$ and $1.6\ W/m^2K$. The convection heat transfer coefficients for model Conic_30 is, $h_{in} = 8.8\ W/m^2K$, $h_r = 8.3\ W/m^2K$. As seen above values, the model of conical domed Harran house (Conic 60) the coefficient for roof outer surface is more than Conic_30. But the most significant difference is between the model Flat and Conic_60, because the Conic_60 's convective heat transfer coefficient is 2.5 times the outer surface value of flat roofed one.

KSÜ Mühendislik Bilimleri Dergisi, 25(2), 2022
Araştırma Makalesi

106

E. Yıldırım

KSU J Eng Sci, 25(2), 2022
Research Article
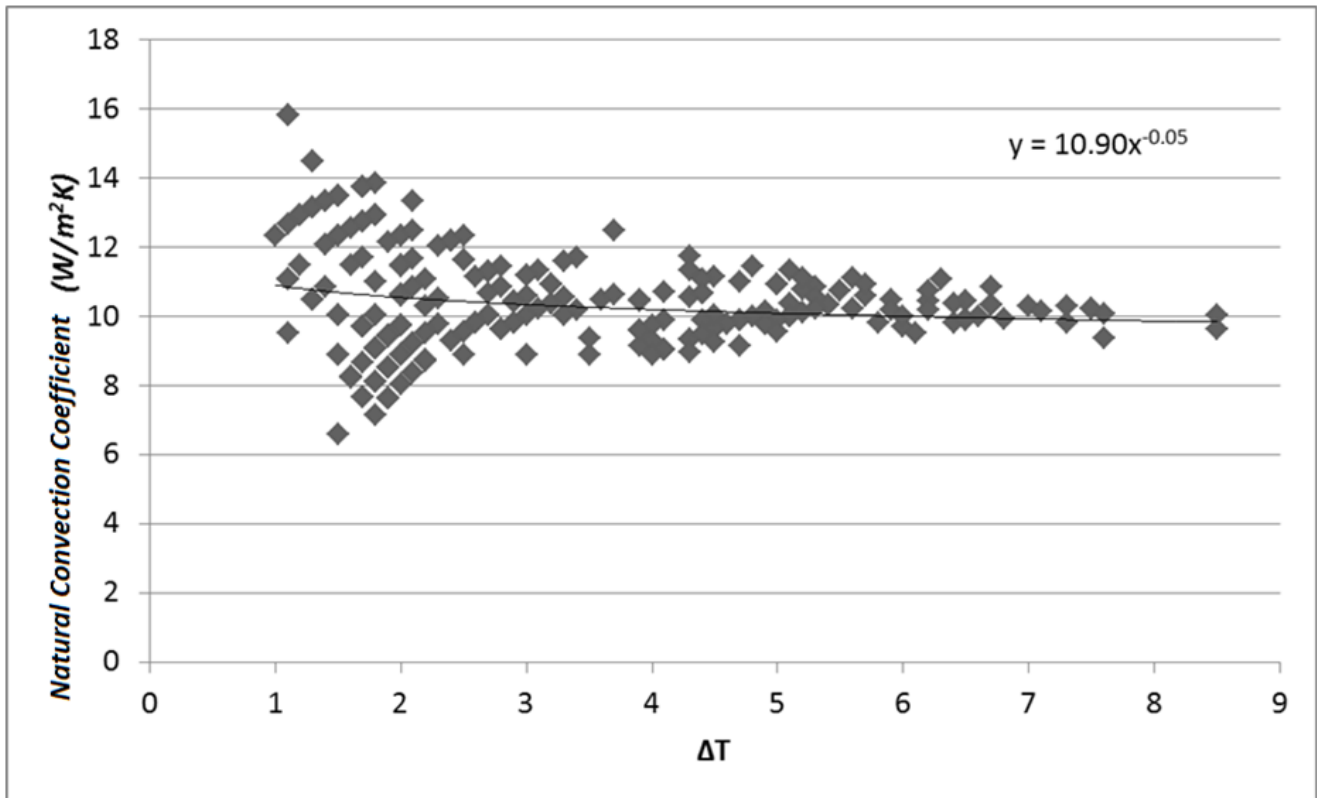
Figure 11 The Variation of The Model Conic_60 Roof Outer Surface Convection Heat Transfer Coefficient As o Function of The Temperature Difference Between The Roof Outer Surface And The Ambient Temperature
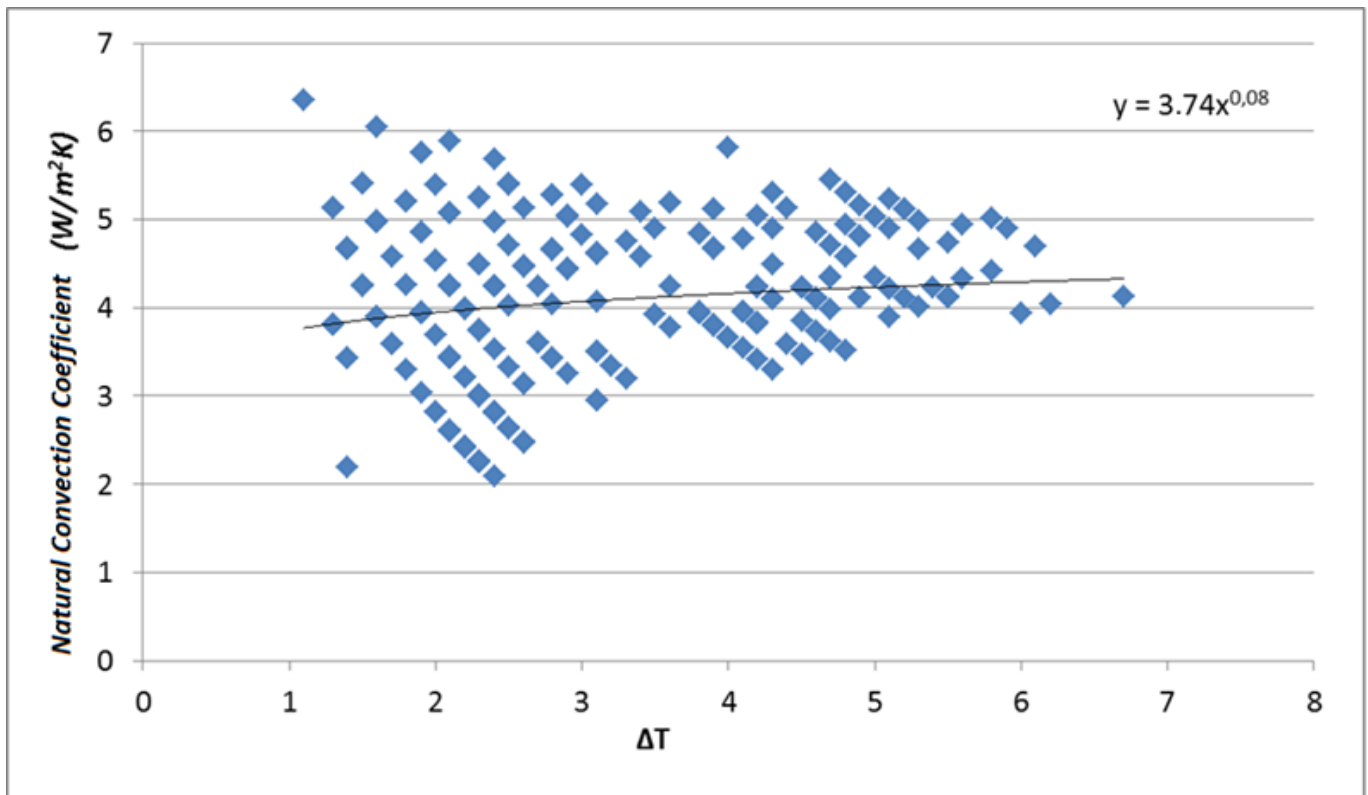
Figure 12 The Variation of The Model Flat Roof Outer Surface Convection Heat Transfer Coefficient as a Function of The Temperature Difference Between the Roof Outer Surface nd The Ambient Temperature

Figure 13 The Variation of The Model Conic_30 Roof Outer Surface Convection Heat Transfer Coefficient as a Function of The Temperature Difference Between the Roof Outer Surface and The Ambient Temperature

CONCLUSION

Conical roofed Harran house model at 1/5 scale (Conic_0) and the equivalent volume and base area of flat roofed model and a model has a roof slope (Conic 30) between these two roof types are used to define the total heat transfer coefficients in terms of changing roof geometry. Also, the natural convection coefficients of the inner volume and the roof outer surfaces of models are compared using experimental and literature data. Experimental results showed that,

Model of conical-roofed Harran house average indoor air temperature is 3.5°C cooler than the flat roofed model indoor air during the experiment at same environmental conditions. For the same base temperature, the roof slope increases the indoor air temperature decreases.

Conical roofed Harran house model has the lowest total thermal resistance from base to roof is and its total heat transfer coefficient is more than 2.5 times the flat roofed model.

It is found that Rayleigh number has an increasing trend with Nusselt number same time. Average convection coefficients calculated with literature correlations are consistent with obtained from experimental data.

Conical roofed Harran house model has the highest inner and outer natural convection coefficients. The average of natural convection heat transfer coefficient of the conical roofed Harran house model roof outer surface is about 1.5 times more than the flat roof model's.

REFERENCES

Acïkgoz, O. (2015). A novel evaluation regarding the influence of surface emissivity on radiative and total heat transfer coefficients in radiant heating systems by means of theoretical and numerical methods. *Energy and Buildings*, 102, 105-116. https://doi.org/10.1016/j.enbuild.2015.05.016.

Basaran T. (2011). Termal analysis of the domed vernacular houses of harran, Turkey. *Indoor and Built Environment*, 20 (5), 543-554.

KSÜ Mühendislik Bilimleri Dergisi, 25(2), 2022
Araştırma Makalesi

108

E. Yıldırım

KSU J Eng Sci, 25(2), 2022
Research Article

Cruickshank, C. A., Harrison, S. J. (2010). Heat loss characteristics for a typical solar domestic hot water storage. *Energy and Buildings*, 42, 1703-1710. https://doi.org/10.1016/j.enbuild.2010.04.013.

Cengel Y. A. (2011). Isı ve Kütle Transferi Pratik bir yaklaşım, 3. Baskı, Güven Bilimsel.

Dalal, A., & Das, M. K. (2006). Natural convection in a rectangular cavity heated from below and uniformly cooled from the top and both sides. *Numerical Heat Transfer, Part A: Applications*, 49:3, 301-322. https://doi.org/10.1080/10407780500343749

Dogan, A., Akkus, S., Baskaya, Ş. (2012). Numerical analysis of natural convection heat transfer from annular fins on a horizontal cylinder. *Isi Bilimi ve Teknigi Dergisi/ Journal of Thermal Science and Technology*, 32. 31-41.

Evangelisti, L., Guattari, C., Gori, P., Bianchi, F. (2017). Heat transfer study of external convective and radiative coefficients for building applications. *Energy and Buildings*. 151, 429–438. https://doi.org/10.1016/j.enbuild.2017.07.004.

François, A., Ibos, L., Feuillet, V., & Meulemans, J. (2020). Novel in situ measurement methods of the total heat transfer coefficient on building walls. *Energy and Buildings*, 219, 110004.

Globe, S. & Dropkin, D. (1959). Natural-convection heat transfer in liquids confined by two horizontal plates and heated from below. *ASME. J. Heat Transfer*, 81(1): 24–28. https://doi.org/10.1115/1.4008124.

Hong, T., Ferrando, M., Luo, X., Causone, F. (2020). Modeling and analysis of heat emissions from buildings to ambient air. *Applied Energy,* 277,115566. https://doi.org/10.1016/j.apenergy.2020.115566.

Hu, Z., Cui, G., Zhang, Z. (2018). Numerical study of mixed convective heat transfer coefficients for building cluster. *Journal of Wind Engineering and Industrial Aerodynamics*, 172, 170-180. https://doi.org/10.1016/j.jweia.2017.10.025.

Iousef, S., Montazeri, H., Blocken, B. (2019). Impact of exterior convective heat transfer coefficient models on the energy demand prediction of buildings with different geometry. *Build. Simul*. 12, 797–816 https://doi.org/10.1007/s12273-019-0531-7.

Jiang, F., Yuan, Y., Li, Z., Zhao, Q., Zhao, K. (2020). Correlations for the forced convective heat transfer at a windward building façade with exterior louver blinds. *Solar Energy*, 209, 709-723. https://doi.org/10.1016/j.solener.2020.07.014.

Kline, S., McClintock, F. (1953). Describing uncertainties in single sample experiments, *Mechanical Engineer* ,75, 3-8.

McAdams, W. H. (1954). Heat Transmission, 3rd Ed. McGraw-Hill, New York, NY.

Montazeri, H., Blocken, B., Derome, D., Carmeliet, J. Hensen, J.L.M. (2015). CFD analysis of forced convective heat transfer coefficients at windward building facades: Influence of building geometry. *Journal of Wind Engineering and Industrial Aerodynamics*, 146, 102-116. https://doi.org/10.1016/j.jweia.2015.07.007.

Montazeri, H. & Blocken, B. (2017). New generalized expressions for forced convective heat transfer coefficients at building facades and roofs. *Building and Environment*, 119, 153-168. https://doi.org/10.1016/j.buildenv.2017.04.012.

Montazeri, H. & Blocken, B. (2018). Extension of generalized forced convective heat transfer coefficient expressions for isolated buildings taking into account oblique wind directions, *Building and Environment*, 140, 194-208. https://doi.org/10.1016/j.buildenv.2018.05.027.

Nogueira, R., Martins, M., Ampessan, F. (2011). Natural convection in rectangular cavities with different aspect ratios. Therm Eng. 10. 44-49. 10.5380/reterm.v10i1-2.61951.

Premrov, M., Žigart, M., Vesna, L. (2017). Influence of the building geometry on energy efficiency of timber-glass buildings for different climatic regions. *Istrazivanja i projektovanja za privredu*. 15, 529-539. https://doi.org/10.5937/jaes15-15256.

Saleh, H. & Hashim, I. (2014). Conjugate heat transfer in rayleigh-bénard convection in a square enclosure. *The Scientific World Journal,* 786102. 10.1155/2014/786102.

Sarris, I.E., Lekakis, I., Vlachos, N.S. (2004). Natural convection in rectangular tanks heated locally from below. *International Journal of Heat and Mass Transfer*, 47, 3549-3563. https://doi.org/10.1016/j.ijheatmasstransfer.2003.12.022.

Turgut, P., Yesilata, B. (2009). Investigation of Thermo-mechanical behaviors of scrap rubber added mortar plate and bricks. *Journal of The Faculty of Engineering and Architecture of Gazi University*, 24 (4): 651–658.

Yang, W., Zhu, X., Liu, J. (2017). Annual experimental research on convective heat transfer coefficient of exterior surface of building external Wall. *Energy and Buildings*, 155, 207-214. https://doi.org/10.1016/j.enbuild.2017.08.075.

Yesilata, B., Turgut, P. (2007). A simple dynamic measurement technique for comparing thermal insulation performances of anisotropic building materials. *Energy and Buildings*, 39(9):1027-1034.

Yildirim, E., Firatoglu A. Z., Yesilata B. (2014). Comparison of the solar insolation on the roof of conic domed harran house and the flat roof. *Isı Bilimi ve Tekniği Dergisi*, 34(2), 123-128.

Yildirim, E., Firatoglu, Z., Yesilata, B., (2017). Çatı geometrisin bina ısıl davranışı üzerindeki etkisinin incelenmesi. *Uludağ University Journal of The Faculty of Engineering*. 22. 187-200. 10.17482/uumfd.330923.